

Platelet Ice under Arctic Pack Ice in Winter

Christian Katlein^{1*}, Volker Mohrholz², Igor Sheikin³, Polona Itkin⁴, Dmitry V. Divine⁵,
Julienne Stroeve^{6,7}, Arttu Jutila¹, Daniela Krampe¹, Egor Shimanchuk³, Ian Raphael⁸,
Benjamin Rabe¹, Ivan Kuznetov¹, Maria Mallet¹, Hailong Liu⁹, Mario Hoppmann¹, Ying-
Chih Fang¹, Adela Dumitrascu¹⁰, Stefanie Arndt¹, Philipp Anhaus¹, Marcel Nicolaus¹,
Ilkka Matero¹, Marc Oggier¹¹, Hajo Eicken¹¹, Christian Haas¹

¹Alfred-Wegener-Institut Helmholtz-Zentrum für Polar- und Meeresforschung, Bremerhaven,
Germany

²Leibniz Institute for Baltic Sea Research, Rostock-Warnemünde, Germany

³Arctic and Antarctic Research Institute, St.Petersburg, Russia

⁴UiT University of Tromsø, Tromsø, Norway

⁵Norwegian Polar Institute, Tromsø, Norway

⁶University College of London, London, United Kingdom

⁷Center for Earth Observation Science, Department of Environment & Geography, University of
Manitoba, Winnipeg, MB, Canada

⁸Thayer School of Engineering, Dartmouth College, Hanover NH, United States of America

⁹Shanghai Jiao Tong University, Shanghai, China

¹⁰University of Gothenburg, Gothenburg, Sweden

¹¹International Arctic Research Center, University of Alaska Fairbanks, Fairbanks AK, United
States of America

*Corresponding author: Christian Katlein (ckatlein@awi.de)

Key Points:

- Extensive observation of platelet ice formation under Arctic winter sea ice
- The sub-ice platelet layer appears to form locally due to seed crystals in ocean surface supercooling.

29
30
31
32
33
34
35
36
37
38
39
40
41
42
43
44
45
46
47
48
49
50
51
52
53
54
55
56
57

Word count = 4500 words

Abstract

The formation of platelet ice is well known to occur under Antarctic sea ice, where sub-ice platelet layers form from supercooled ice shelf water. In the Arctic however, platelet ice formation has not been extensively observed and its formation and morphology currently remain enigmatic. Here, we present the first comprehensive, long-term in situ observations of a decimeter thick sub-ice platelet layer under free-drifting pack ice of the Central Arctic in winter. Observations carried out with a remotely operated underwater vehicle (ROV) during the midwinter leg of the MOSAiC drift expedition, provide clear evidence of the growth of platelet ice layers from supercooled water present in the ocean mixed layer. This platelet formation takes place under all ice types present during the surveys. Oceanographic data from autonomous observing platforms lead us to the conclusion that platelet ice formation is a widespread but yet overlooked feature of Arctic winter sea ice growth.

Plain language summary

Platelet ice is a particular type of ice that consists of decimeter sized thin ice plates that grow and collect on the underside of sea ice. It is most often related to Antarctic ice shelves and forms from supercooled water with a temperature below the local freezing point. Here we present the first comprehensive observation of platelet ice formation in freely drifting pack ice in the Arctic in winter during the international drift expedition MOSAiC. We investigate its occurrence under the ice with a remotely controlled under-ice diving robot. Measurements of water temperature from automatic measurement devices distributed around the central MOSAiC ice floe show, that supercooled water and thus platelet ice occurs widely in the winter Arctic. This way of ice formation in the Arctic has been overlooked during the last century, as direct observations under winter sea ice were not available and contrary to typical Antarctic observations, manifestation of platelet ice in Arctic ice core stratigraphy has been more challenging to identify.

58 **1. Introduction**

59 Platelet ice is a characteristic feature of Antarctic landfast sea ice, where supercooled ice
60 shelf waters lead to the advection and growth of sub-ice platelet layers [Hoppmann *et al.*, 2020].
61 They consist of loosely attached decimeter sized plate-shaped ice crystals [Hoppmann *et al.*,
62 2017; Langhorne *et al.*, 2015; Smith *et al.*, 2001] and can be up to several meters thick. These ice
63 platelets form by nucleation in supercooled layers of seawater either at depth [Dieckmann *et al.*,
64 1986] or directly at the ice underside [Leonard *et al.*, 2006; Mahoney *et al.*, 2011] in the vicinity
65 of large ice shelves, which provide supercooled water due to basal ice shelf melt in the water
66 circulation of ice shelf cavities. The porous structure provides shelter for a particular ice
67 associated ecosystem [Arrigo *et al.*, 2010; Günther and Dieckmann, 2004; Vacchi *et al.*, 2012]
68 and is thus important for biogeochemical cycles [Thomas and Dieckmann, 2002].

69 As ice shelves are much less common in the Arctic [Dowdeswell and Jeffries, 2017],
70 observations of platelet ice in the Arctic are rare and the processes causing its formation are
71 poorly understood. The availability of supercooled water plays a central role for the growth of
72 decimeter scale ice platelets [Lewis and Perkin, 1983; 1986; Weeks and Ackley, 1986]. Jeffries *et al.*
73 [1995] presented one of the few descriptions of platelet ice in the Arctic Ocean. Their study
74 identified platelet ice crystals in 22 out of 57 ice cores collected in the Beaufort Sea during
75 August and September 1992 and 1993. They suggest four different sources for supercooled
76 water, two of which require the presence of ice shelves and coastal interactions and are therefore
77 not relevant for the central Arctic Ocean. The other two include small scale “ice pump”
78 mechanisms [Lewis and Perkin, 1983; 1986] and the interaction of summer meltwater with the
79 underlying colder seawater, leading to the formation of false bottoms in under-ice melt ponds
80 and platelet ice crystals [Eicken, 1994; Martin and Kauffman, 2006; Notz *et al.*, 2003]. They
81 describe platelet ice as a widespread feature in the Beaufort Sea based on their ice-core analysis.
82 Carnat *et al.* [2017] describe two cores with platelet ice signature. Early observations from Lewis
83 and Lake [1971] stay vague in the description, but show that the phenomenon is not new. The
84 Russian drifting station NP-2015 also detected platelet formation caused by meltwater
85 percolation through the ice cover (personal communication I. Sheikin) and an indirect
86 observation under fast ice in summer was described by Kirillov *et al.* [2018].

87 Sub-ice platelet layers can be separated from frazil ice in such way that the geometric
88 size of the platelet ice crystals is on the order of 1-10 cm. Frazil ice describes the crystal habit

89 resulting from the initial stages of sea-ice growth, when small disk and needle-like crystals
90 smaller than 1 cm appear suspended in the upper water column or at the ocean surface
91 [Hoppmann *et al.*, 2020; Weeks and Ackley, 1986; Zubov, 1963]. Sub-ice platelet layers exhibit a
92 rather random orientation of crystal axes. This is significantly different from the skeletal layer at
93 the bottom of growing sea ice, where parallel oriented ice lamellae are growing into a microscale
94 layer of constitutionally supercooled water caused by the brine expulsion during sea-water
95 freezing [Lofgren and Weeks, 2017; Rutter and Chalmers, 1953; Shokr and Sinha, 2015].

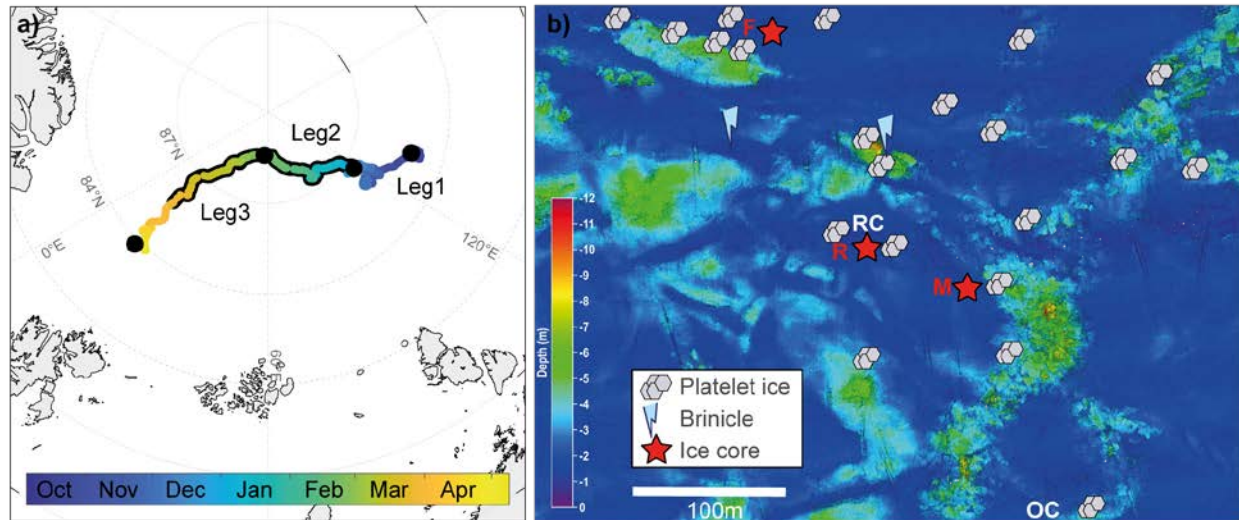
96 No extensive direct in situ observations of platelet ice under Arctic sea ice particularly
97 during winter are available. Anecdotal reports from divers, such as during the Tara expedition
98 [Ragobert *et al.*, 2008] or the “Under the Pole” diving expedition [Bardout *et al.*, 2011], allude
99 that this feature has been mostly overlooked in the Central Arctic. Figure S1 and Table ST1
100 provide an overview of previous observations.

101 Here, we present the first extensive, more systematic in situ observations of growing sub-
102 ice platelet layers under Arctic sea ice in winter. Dives with a remotely operated vehicle during
103 the international Arctic drift expedition “Multidisciplinary Observatory for the Study of Arctic
104 Climate” (MOSAiC) from January to March 2020 around 88°N (Figure 1) revealed a widespread
105 coverage of decimeter scale platelet ice crystals growing on and under the bottom of the ice.

106 **2. Materials and Methods**

107 **2.1 Study Area**

108 The ice floe of the MOSAiC drift experiment of the German research icebreaker
109 Polarstern [Knust, 2017] consisted of a conglomerate of various ice types, out of which deformed
110 second year ice and relatively level residual ice (first year ice grown into a remaining matrix of
111 very rotten melted ice [WMO, 2014]) were the most abundant. Initial ice thicknesses during the
112 mobilization of the drift station in the beginning of October 2019 were as little as 20-30 cm for
113 the residual ice and around 60-80 cm for the undeformed second year ice [Krumpen *et al.*, 2020].
114 By March, ice growth had increased the level ice thickness to about 145 cm for the residual ice
115 and around 200 cm for the second year ice (Figure S2). Pressure ridges with typical keel drafts of
116 5-7 m and maximum of 11 m characterized the deformed ice. More details about the composition
117 and history of the MOSAiC floe can be found in Krumpen *et al.* [2020].



118

119 **Figure 1.** a) Drift track of MOSAiC floe in the Central Arctic Ocean from October 2019 to mid-
 120 May 2020. Black dots denote start and end of drift legs 1, 2 and 3, respectively. Platelet ice was
 121 observed between 30 December 2019 and 28 March 2020 (black highlighted track). b) Map of
 122 ice draft derived from multibeam sonar survey on 21 January 2020 with most prominent
 123 locations of the ubiquitous platelet ice observations (grey symbols), brinicles (light blue
 124 symbols) and ice core samples (red stars). White letters indicate the position of the ROV access
 125 hole (RC) and the MSS deployment hole (OC). Red letters refer to ice cores taken at the ROV
 126 site (R), the ice mechanics site (M) and the ridge site (F).

127 2.2 ROV Operations

128 We carried out remotely operated vehicle (ROV) dives from a hole through the ice
 129 covered by a heated tent. The M500 ROV (Ocean Modules, Atvidaberg, Sweden) was equipped
 130 with a comprehensive sensor suite including cameras as well as a 240 kHz multibeam sonar
 131 [Katlein *et al.*, 2017] and provided an operating range of 300 m from the access hole. We
 132 documented platelet ice occurrences mostly with four cameras: a high definition zoom video
 133 camera (Surveyor HD, Teledyne Bowtech, Aberdeen, UK), two standard definition video
 134 cameras (L3C-720, Teledyne Bowtech, Aberdeen, UK) and a 12 megapixel still camera (Tiger
 135 Shark, Imenco AS, Haugesund, Norway).

136 The ROV dives covered many different sites, but several places were revisited (Figure
 137 1b) due to repeating routine dive missions allowing for a temporal assessment of platelet ice
 138 evolution. On 15 February 2020, we towed an under-ice zooplankton net (ROVnet) with the
 139 ROV directly along the ice underside [Wollenburg *et al.*, 2020] to brush off platelet ice samples
 140 for structural analysis. In the lab, platelets were frozen into a solid block of ice by adding sea
 141 water to the sample container, in order to later analyze the platelet ice crystal structure.

142 **2.3 Ice Core Sampling and Analysis**

143 We extracted ice cores in three locations (Figure 1b) where sub-ice platelet coverage had
144 been previously confirmed by ROV imagery. We analyzed them for ice texture by preparing thin
145 sections using the Double Microtoming Technique [*Eicken and Salganek, 2010; Shokr and*
146 *Sinha, 2015*] in the lab on board. We photographed the thin sections between crossed polarizers
147 to identify crystal geometric properties. To associate an approximate date of ice formation to
148 each ice sample along the core, we used a simple ice-growth model based on the number of
149 freezing-degree-days [*Pfirman et al., 2004*], forced by air temperatures recorded by the
150 Polarstern weather station.

151 **2.4 Physical Oceanographic Measurements**

152 We measured vertical and horizontal profiles of seawater conductivity, temperature, and
153 pressure (CTD) using three independent different types of platforms. One CTD sensor was
154 mounted on the ROV (GPCTD, SeaBird Scientific, USA), while we performed recurring
155 deployments of a free-falling microstructure sonde (MSS 90LM, Sea and Sun Technologies,
156 Trappenkamp, Germany) through a nearby hole in the ice (Figure 1b). In addition, several
157 autonomous stations with CTD packages at a depth of 10 m (SBE37, SeaBird Scientific, USA)
158 were operational in the MOSAiC distributed network at distances of 10-40 km from the central
159 floe (Figure S3). All devices were calibrated by the manufacturers immediately before the
160 expedition. The respective measurement uncertainties are discussed in supplementary text T1.

161 **3. Results and Discussion**

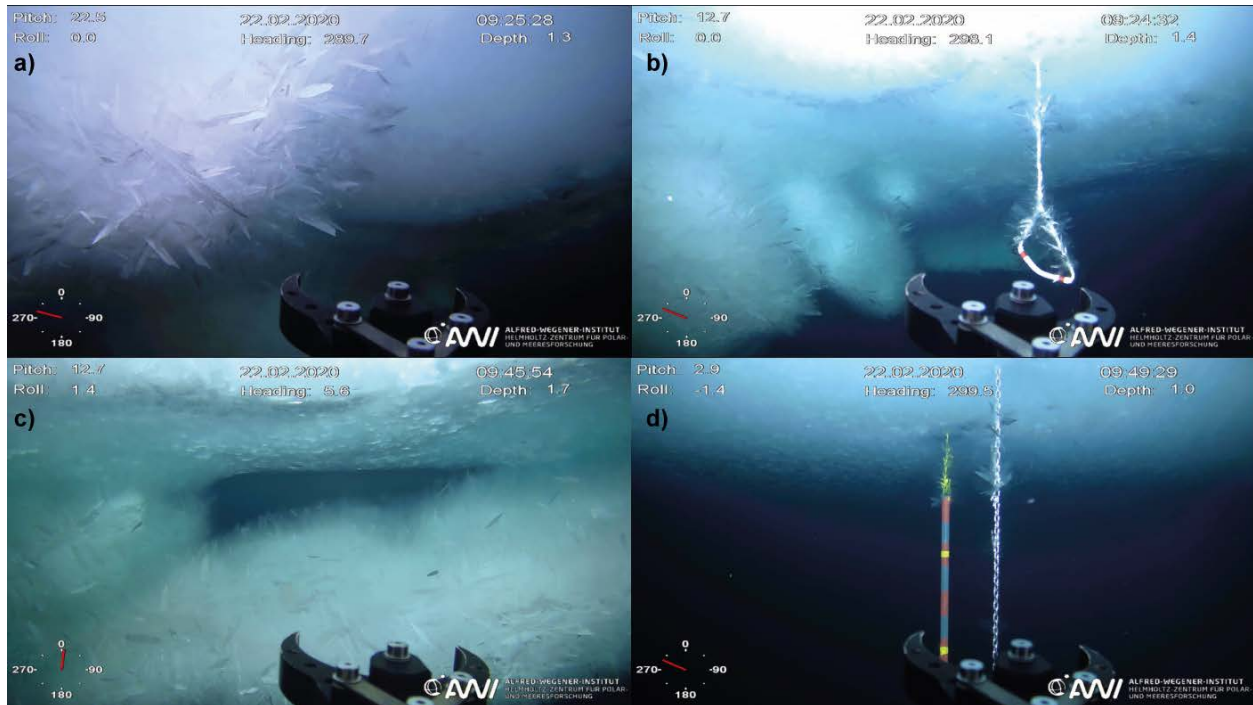
162 **3.1 Sub-ice Platelet Layer Morphology**

163 We observed a 5 to 30 cm thick sub-ice platelet layer covering the ice bottom as shown in
164 Figure 2. The ice platelets are composed of blade- or disc-shaped single ice crystals with c-axis
165 alignment normal to the platelet surface. Most platelets were firmly attached to their substrate
166 but fragile to physical impact by the ROV. When observed on ropes or chains, platelet ice
167 crystals were tightly grown through their structure (Figures 2b, S4) and not just loosely attached
168 to the respective surface. This indicates that these platelets grew on site and have not been
169 advected in from deeper waters or horizontally as already suggested by *Lewis and Lake [1971]*.
170 Contrary to Antarctic fast ice, we did not find meter thick layers of platelet ice accumulation
171 [*Hoppmann et al., 2017; Hunkeler et al., 2016*], possibly due to slower platelet or faster

172 congelation growth. The freezing front of the congelation ice quickly progressed downward into
173 the sub-ice platelet layer and incorporated it by congelation ice growth in between the platelet
174 crystals [Dempsey *et al.*, 2010]. A thickness difference between Arctic and Antarctic sub-ice
175 platelet layers was already proposed by Lewis and Perkin [1986] based on different driving
176 depths in the ice pump mechanism.

177 We identified crystal sizes up to approximately 15 cm from the ROV camera footage.
178 Maximum crystal size retrieved with the towed zooplankton net was 9 cm, while the thicknesses
179 of platelet crystals ranged from 0.8-2.5 mm. However, due to the limited size of the sampling
180 bottle with a diameter of 10 cm and the physical interaction of the ROVnet (0.4 by 0.6 m
181 opening) and platelet ice structures, platelets may well have been broken during the sampling
182 process.

183 Platelet ice growth depends on available crystallization nuclei or seed crystals for
184 secondary nucleation. Probably due to this reason, we did not observe platelet growth on the
185 polymer-covered thermistor strings hanging in the water column. The complex structure of core-
186 mantle polyamide rope or metal parts provided sufficient crystallization nuclei for platelet
187 formation (Figures 2d, S4). Another explanation could be material dependent adhesion of seed
188 crystals as described in Robinson *et al.* [2020]. This was particularly obvious on 15 February
189 2020, when the ROV had been hanging for three days in 2 m water depth and was covered in up
190 to 30 mm large platelet crystals on edges and corners, while particularly smooth plastic surfaces
191 were unaffected by platelet growth (Figure S5).



192

193 **Figure 2.** a) Close-up picture of platelet ice covering a ridge block. The ROV manipulator
 194 opening in the foreground is about 9 cm wide. b) Rope sling next to a pressure ridge: both, the
 195 rope and the ridge are vastly covered in ice platelets. c) Upward growing platelet ice in a ridge
 196 cavity. d) Platelet ice crystals covering the rope and chain of underwater installations. Note the
 197 lack of platelet growth on the plastic marker stick and the coverage of small platelet crystals
 198 underneath the level ice.

199

3.2 Spatial Distribution of Platelets

200

Platelet ice coverage was ubiquitous in the entire observational range of the ROV.

201

However, platelet ice growth was almost exclusively observed in the uppermost part of the water

202

column, above a depth of 2-3 m. Deeper lying ridge keels as well as deep hanging ropes and

203

instrument installations were not covered in platelet ice. Few installations exhibited a vertical

204

gradient of platelet ice growth coverage, with the most extensive occurrence at the ice-water

205

interface and diminishing platelet cover towards depth (Figure S6). This has been observed

206

similarly in the Antarctic [Dayton *et al.*, 1969; Hoppmann *et al.*, 2020; Mahoney *et al.*, 2011].

207

Platelet crystals were largest (up to 15 cm) and most prominent on blocks, ridges, and edges

208

protruding from the level ice, but at close inspection, we found also smaller scale platelet ice

209

crystals (1-2 cm) throughout the bottom of level ice. Also these smaller platelets appeared

210

different from ice lamellae expected in the skeletal layer. We identified no significant spatial

211 difference in under-ice roughness (and thus platelet coverage) from acoustic backscatter derived
212 from the multibeam sonar measurements (Figure S7).

213 While sheltered areas between ridge keels with low currents seemed to provide best
214 conditions for platelet growth, we observed significant platelet growth of similar size also at
215 locations that were completely exposed to the ice-relative currents (Figure S4) and more than
216 100m away from any significant ice feature. *Lewis and Milne* [1977] attribute the presence of
217 sub-ice platelet layers to cracks or pressure ridges. While this seems to coincide with the
218 locations of our most prominent observations, we also observed platelet ice far away from such
219 features and can thus neither prove nor rule out the ridge associated ice-pump mechanism of
220 platelet formation as predicted by *Lewis and Perkin* [1986].

221 We found no direct link between platelet ice distribution and brine drainage features.
222 Despite the occasional observation of brinicles – ice stalactites forming from the contact of
223 descending, cold brine with seawater [*Lewis and Milne, 1977*]- we encountered them both with
224 and without intense platelet ice cover (Figure S8).

225 **3.3 Temporal Variability**

226 During MOSAiC, the ROV diving schedule only allowed for a weekly cycle of repeated
227 visits (Figure S9). Therefore, our information on the temporal variability of platelet ice
228 occurrence is limited and less objective. However, we could identify clear differences in the
229 amount of new platelet ice formation between different periods. These periods were
230 characterized either by new crystal growth, the lack of such, or even a perceived reduction in
231 platelet ice cover. They are identified in Figure 3 to investigate a link between oceanographic
232 conditions and platelet ice formation. As the ROV sampling in the described location only
233 started on 31 December 2019, we cannot provide a detailed assessment of the situation before.
234 However, we observed no platelet ice during ROV dives before 6 December 2019 in a different
235 location approximately 1 km away. We observed platelet ice for the last time during an ROV
236 dive on 28 March 2020, after the floe had been affected by deformation and the return of
237 sunlight. This coincides with the time, when water temperatures under the ice climbed above the
238 local freezing point again (Figure 3c).

239 **3.4 Supercooling**

240 We found supercooled water, the basis for platelet ice formation, well below the ice-
241 water interface, which we confirmed using three different independent measurement platforms.
242 Temperature and salinity data from the ROV, a free-falling Microstructure Sonde (MSS), and
243 several autonomous CTDs deployed at 10 m depth in 10-40 km distance from the ROV site all
244 revealed water temperatures around 0.01-0.02 K below the respective seawater freezing point in
245 the uppermost mixed layer (Figure 3a). This degree of supercooling is similar to observations
246 from the Antarctic [Mahoney *et al.*, 2011] and larger than the calibration uncertainty and
247 uncertainties in the calculation of the local freezing point of seawater. Hence, we can confirm the
248 existence of supercooled water several meters thick as prerequisite for platelet ice formation
249 [Smith *et al.*, 2001]. Measurement uncertainties might however obscure the absolute magnitude
250 and depth of ocean surface supercooling.

251 Within the mixed layer, the local seawater freezing point is pressure and therefore depth
252 dependent, while temperature and salinity values are approximately constant. Thus, freezing-
253 point departure increases towards the surface with a higher level of supercooling in the
254 uppermost mixed layer right under the ice (Figure 3a,b). This can explain the observed decrease
255 in platelet ice abundance below 2 m depth.

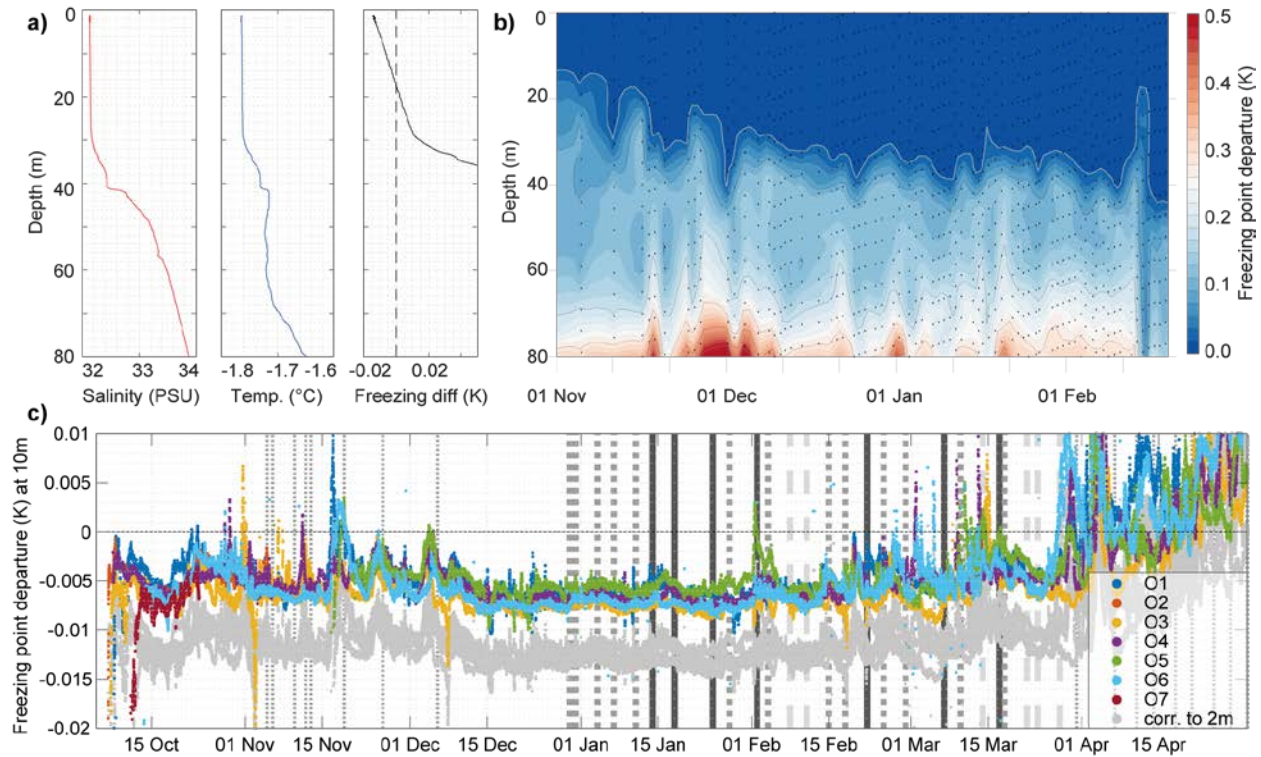
256 A simple hypothesis for platelet ice growth might thus be that water molecules attach to
257 existing crystallization nuclei e.g. at the ice underside as soon as they are in a strong enough state
258 of supercooling. Considering the turbulent nature of the mixed layer, where water particles get
259 mixed up and down through the entire mixed layer at a time scale of 30 minutes [Denman and
260 Gargett, 1983], they oscillate between supercooled and non-supercooled states. Thus, we
261 hypothesize that platelet ice formation is only possible as soon as the temperature in the
262 complete mixed layer lies below the vertically averaged seawater freezing point. This can be
263 either achieved by excessive atmospheric cooling during the Arctic winter [Danielson *et al.*,
264 2006; Skogseth *et al.*, 2017] or due to a sudden shoaling of the mixed layer, cutting off mixing
265 beyond a certain depth, so that suddenly most of the surface mixed layer has a temperature below
266 the freezing point causing respective formation of platelet ice. Platelet ice could also originate
267 from frazil crystals generated in the water column [Robinson *et al.*, 2020; Skogseth *et al.*, 2017]
268 that rise up and attach to the surface. If present, free floating frazil ice crystals should have been
269 easily detected in light beams used for ROV surveys or Secchi-disk casts. No such enhanced

270 light-scattering by ice crystals was observed but we might have missed it particularly due to
271 temporal limitations of the sampling schedule. Another plausible explanation for platelet
272 formation, lies in the “ice-pump” mechanism [Lewis and Perkin, 1983; 1986]: Descending salty
273 brines generated by strong atmospheric cooling in leads or even under a completely closed ice
274 cover can melt deep lying ridge keels and thus supercool the water column and respectively
275 generate platelet ice. Determining the exact nature of the processes involved in the temporally
276 varying strength of platelet ice formation would require more targeted high temporal resolution
277 investigations of platelet growth than could be accomplished during the rigid observational plan
278 for MOSAiC.

279 Time series of MSS and autonomous observations show that the detected levels of
280 platelet ice were only apparent after a more temporally stable mixed layer with a depth of ~30 m
281 had established in mid-December. Furthermore, the perceived decrease in platelet ice coverage
282 observed in mid-February was likely linked to a passing eddy, decreasing the freezing-point
283 departure in the upper mixed layer (Figure 3b).

284 Observations of autonomous CTD sensors deployed in the distributed network at 10 to 40
285 km distance from the central MOSAiC floe (Figure S3) consistently show similar amounts of
286 ocean surface supercooling (Figure 3c). This allows the conclusion that platelet ice formation
287 under Arctic winter sea ice is not a local curiosity, but a widespread, overlooked feature in the
288 Central Arctic Ocean.

289



290

291 **Figure 3.** a) Salinity, temperature, and freezing point departure observed by the ROV on 22
 292 February 2020. b) MSS time series of water temperature above the surface freezing point. Note
 293 the consistent deepening of the supercooled layer indicated in blue color. c) Time series of
 294 freezing-point departure measured in 10 m depth (and adjusted to 2 m depth in gray) from the
 295 autonomous observation stations. Vertical lines indicate platelet ice intensity observations
 296 classified as high (solid lines), normal (thick dotted lines) and low intensity (dashed lines) based
 297 on visual ROV observations. Thin dotted lines indicate ROV surveys without platelet ice
 298 observation. See supplemental figure S3 for geometric location of stations relative to the central
 299 observatory.

300 3.5 Persistence in Ice Core Analysis

301 Despite the ubiquitous occurrence of platelet ice shown in our study, there is a general
 302 lack of extensive signs of platelet ice formation in the texture of Arctic sea ice cores of the
 303 Transpolar Drift [Tucker *et al.*, 1999]. To further investigate, we retrieved ice cores at three
 304 locations (Figure 1b) where we had documented platelet ice beforehand with the ROV cameras.
 305 In contrast to most Antarctic landfast ice cores, all of the investigated ice core bottom thin
 306 sections (Figure S10) showed only weak signs of incorporated platelet ice. Rapid congelation ice
 307 growth of 5-9 cm per week might have concealed a more obvious signature of platelets
 308 [Dempsey *et al.*, 2010; Gough *et al.*, 2012]. However, in various places we found a few large,

309 inclined crystals interpreted as originating from platelet crystals. Moreover, during the first leg of
310 MOSAiC at the end of November 2019, an ice core retrieved at the second-year ice site
311 contained more clearly identifiable sections of platelet ice (Figure S11). Thin section analysis
312 indicates substantial microstructural and textural similarities with literature reports of Antarctic
313 platelet ice [Jeffries *et al.*, 1995; Langhorne *et al.*, 2015; Leonard *et al.*, 2006; Smith *et al.*,
314 2001].

315 To investigate this more closely, we analyzed the texture of collected platelet crystals
316 refrozen into seawater. The resulting texture (Figure S12) looks significantly different from the
317 one described for freshwater-derived platelet ice by Jeffries *et al.* [1995]. In particular, platelet
318 ice crystals seen from the side have a rectangular rather than triangular shape, and also many
319 platelet crystals exhibit sub-grain boundaries which are described as absent in the work of
320 Jeffries *et al.* [1995].

321 We thus have two hypotheses why these ubiquitous platelet ice crystals under Arctic
322 winter sea ice do not leave a strong record in the texture of ice cores. First, despite their
323 spectacular voluminous appearance, the ice platelets actually only take up a small volume
324 fraction, so that it is unlikely to observe multiple platelet crystals in a sub-millimeter thick ice
325 core thin section. This has been found also for Antarctic platelet ice incorporated into fast
326 growing congelation ice [Dempsey *et al.*, 2010; Gough *et al.*, 2012]. Second, the platelet crystals
327 may serve as primary nucleation surfaces also for the congelation growth in a way that obscures
328 their initial origin. Both hypotheses could explain why such a widespread cover of sub-ice
329 platelet layers in the winter Arctic has been overlooked in the last decades of sea ice texture
330 investigations.

331 **3.6 Physical, Ecological and Biogeochemical Implications**

332 Considering large scale energy fluxes and the thermodynamics of sea ice growth, platelet
333 ice formation under Arctic sea ice in winter does likely not affect the thermodynamics of sea ice
334 growth significantly. This is particularly due to Arctic platelet ice being a local seasonal
335 phenomenon maintaining a closed energy budget. In contrast, Antarctic platelet ice is often
336 derived from water masses with spatially different origin and thus disrupting the local energy
337 budget. Even though the impact may be small for ice-ocean physics, the porous, ragged structure
338 of the platelet ice interface does affect small scale roughness of the ice underside and will in

339 particular affect the entrainment of water constituents, such as sediments, nutrients, or biological
340 assemblages. One sample of sub-ice platelets from the ROVnet showed elevated levels of
341 halocarbons compared to the general ice column, meaning this sub-ice platelet layer could play a
342 role also in different biogeochemical cycles. Despite the assumed inactivity of the under-ice
343 ecosystem during polar night, platelet ice might still serve as a substrate for algal growth and
344 protection for under-ice macrofauna, as we observed amphipods maneuvering through the maze
345 of crystal blades (Figure S13).

346 Platelet ice could also play a significant role in the poorly understood consolidation of
347 voids e.g. in sea ice ridges, where it would be able to close large gaps faster than by pure
348 congelation ice growth. This could explain why voids in ridge keels often appeared slushy when
349 drilled through during MOSAiC (Figure S14).

350 While platelet ice observations in the Arctic date back to the 1970s [*Lewis and Milne,*
351 1977], the thinner [*Haas et al., 2008; Kwok and Rothrock, 2009*] and more dynamic sea ice
352 [*Kwok et al., 2013*] of recent years might increase rapid cooling of Arctic surface waters and thus
353 promote platelet ice formation.

354 **4. Summary**

355 During the polar night of the international drift expedition MOSAiC in 2019-2020, we
356 observed a widespread coverage of the ice underside with a sub-ice platelet layer. These up to 15
357 cm large platelet ice crystals grew in situ from supercooled water of the uppermost mixed-layer,
358 both on exposed ice features and level ice. This is the first comprehensive in situ observation of
359 sub-ice platelet layer formation during Arctic winter in the free-drifting ice of the Central Arctic.
360 As historic observations show, this is not a new phenomenon but only modern robotic equipment
361 at a winter drift ice station allowed for its detailed observation.

362 Platelet ice formation has been overlooked so far as a widespread feature of ice growth
363 during Arctic winter. Our study provides the first observational evidence for a link between
364 platelet growth intensity, mixed layer stability and supercooling, but the detailed processes with
365 respect to their seasonal impacts on ice-ocean interactions are yet to be understood. In particular,
366 we were able to show that this sub-ice platelet layer does not always leave a clear imprint on sea-
367 ice texture and was hence easily overlooked in past ice core analyses (Figure S15).

368 The potential importance of sub-ice platelet layers for the ice-associated ecosystem and
369 biogeochemical fluxes during Arctic winter should be investigated more closely in the future. To
370 improve our understanding of the involved physical processes, we suggest a more targeted
371 investigation during future Arctic winter campaigns with the goal to achieve higher temporal
372 resolution and more objective observations of platelet crystal growth. This could be achieved by
373 fixed underwater cameras in relation to water dynamics, potential ridge keel melting and
374 thermodynamics in the mixed layer.

375 **Data availability statement**

376 Data used in this manuscript were produced as part of the international Multidisciplinary
377 drifting Observatory for the Study of the Arctic Climate (MOSAiC) with the tag
378 MOSAiC20192020. All data is archived in the MOSAiC Central Storage (MCS) and will be
379 available on PANGAEA after finalization of the respective datasets according to the MOSAiC
380 data policy. Screenshots from ROV video [Katlein *et al.*, 2020d], acoustic backscatter [Katlein *et*
381 *al.*, 2020b], ice core data [Katlein *et al.*, 2020c] and ROV CTD data [Katlein *et al.*, 2020a] are
382 already available on PANGAEA. Oceanographic data from autonomous platforms 2019O1-
383 201908 can be accessed at seaiceportal.de. Ice and snow thickness data were kindly provided by
384 Stefan Hendricks.

385 **Acknowledgments**

386 We are thankful to all members of the MOSAiC collaboration who made this unique
387 expedition possible. We want to thank all people enabling the MOSAiC ROV and buoy
388 programs at AWI, in particular Julia Regnery, Kathrin Riemann-Campe, Martin Schiller, Anja
389 Nicolaus, Dirk Kalmbach. Furthermore, we thank Johannes Lemburg from the AWI workshop
390 and Hauke Flores for providing the ROVnet. We also thank the Captain, Crew and Chief
391 Scientists of RV Polarstern and support icebreakers IB Kapitan Dranitsyn and RV Akademik
392 Fedorov for their support (Project ID: AWI_PS122_00). The participation of Dmitry V. Divine
393 in the MOSAiC expedition was supported by Research Council of Norway project HAVOC (No.
394 280292) and project DEARice supported by EU ARICE program (EU grant agreement No.
395 730965). Participation of Ilkka Matero was supported by the Diatom ARCTIC project (BMBF
396 grant, 03F0810A), part of the Changing Arctic Ocean programme, jointly funded by the UKRI
397 Natural Environment Research Council (NERC) and the German Federal Ministry of Education

398 and Research (BMBF). Stefanie Arndt was funded by the German Research Council (DFG) in
 399 the framework of the priority program “Antarctic Research with comparative investigations in
 400 Arctic ice areas” by grant to SPP1158. We thank one anonymous reviewer and Pat Langhorne
 401 for improving this manuscript during the peer-review process.

402 This study was funded by the Alfred-Wegener-Institut Helmholtz-Zentrum für Polar- und
 403 Meeresforschung and the Helmholtz Research program PACES II. Operation and development
 404 of the ROV were supported by the Helmholtz Infrastructure Initiative “Frontiers in Arctic
 405 Marine Monitoring (FRAM)”.

406 **References**

- 407
 408 Arrigo, K. R., T. Mock, and M. P. Lizotte (2010), Primary Producers and Sea Ice, in *Sea Ice*,
 409 edited by D. G. S. Thomas N.D. , pp. 283-325, doi:10.1002/9781444317145.ch8.
- 410 Bardout, G., E. Périé, and B. Poyelle (2011), *On a marché sous le pôle : Deepsea under the Pole*,
 411 Chêne, [Paris].
- 412 Carnat, G., T. Papakyriakou, N. X. Geilfus, F. Brabant, B. Delille, M. Vancoppenolle, G. Gilson,
 413 J. Zhou, and J.-L. Tison (2017), Investigations on physical and textural properties of Arctic first-
 414 year sea ice in the Amundsen Gulf, Canada, November 2007–June 2008 (IPY-CFL system
 415 study), *J. Glaciol.*, 59(217), 819-837, doi:10.3189/2013JoG12J148.
- 416 Danielson, S., K. Aagaard, T. Weingartner, S. Martin, P. Winsor, G. Gawarkiewicz, and D.
 417 Quadfasel (2006), The St. Lawrence polynya and the Bering shelf circulation: New observations
 418 and a model comparison, *Journal of Geophysical Research: Oceans*, 111(C9),
 419 doi:10.1029/2005jc003268.
- 420 Dayton, P. K., G. A. Robilliard, and A. L. Devries (1969), Anchor Ice Formation in McMurdo
 421 Sound, Antarctica, and Its Biological Effects, *Science*, 163(3864), 273-274,
 422 doi:10.1126/science.163.3864.273.
- 423 Dempsey, D. E., P. J. Langhorne, N. J. Robinson, M. J. M. Williams, T. G. Haskell, and R. D.
 424 Frew (2010), Observation and modeling of platelet ice fabric in McMurdo Sound, Antarctica,
 425 *Journal of Geophysical Research: Oceans*, 115(C1), doi:10.1029/2008jc005264.
- 426 Denman, K. L., and A. E. Gargett (1983), Time and space scales of vertical mixing and
 427 advection of phytoplankton in the upper ocean, *Limnol. Oceanogr.*, 28(5), 801-815,
 428 doi:10.4319/lo.1983.28.5.0801.
- 429 Dieckmann, G., G. Rohardt, H. Hellmer, and J. Kipfstuhl (1986), The occurrence of ice platelets
 430 at 250 m depth near the Filchner Ice Shelf and its significance for sea ice biology, *Deep Sea*
 431 *Research Part A. Oceanographic Research Papers*, 33(2), 141-148,
 432 doi:[https://doi.org/10.1016/0198-0149\(86\)90114-7](https://doi.org/10.1016/0198-0149(86)90114-7).

- 433 Dowdeswell, J. A., and M. O. Jeffries (2017), Arctic Ice Shelves: An Introduction, in *Arctic Ice*
 434 *Shelves and Ice Islands*, edited by L. Copland and D. Mueller, pp. 3-21, Springer Netherlands,
 435 Dordrecht, doi:10.1007/978-94-024-1101-0_1.
- 436 Eicken, H. (1994), Structure of under-ice melt ponds in the central Arctic and their effect on, the
 437 sea-ice cover, *Limnol. Oceanogr.*, *39*(3), 682-693, doi:10.4319/lo.1994.39.3.0682.
- 438 Eicken, H., and M. Salganek (2010), *Field Techniques for Sea-Ice Research*, University of
 439 Alaska Press.
- 440 Gough, A. J., A. R. Mahoney, P. J. Langhorne, M. J. M. Williams, N. J. Robinson, and T. G.
 441 Haskell (2012), Signatures of supercooling: McMurdo Sound platelet ice, *J. Glaciol.*, *58*(207),
 442 38-50, doi:10.3189/2012JoG10J218.
- 443 Günther, S., and G. S. Dieckmann (2004), Seasonal development of algal biomass in snow-
 444 covered fast ice and the underlying platelet layer in the Weddell Sea, Antarctica, *Antarctic*
 445 *Science*, *11*(3), 305-315, doi:10.1017/S0954102099000395.
- 446 Haas, C., A. Pfaffling, S. Hendricks, L. Rabenstein, J.-L. Etienne, and I. Rigor (2008), Reduced
 447 ice thickness in Arctic Transpolar Drift favors rapid ice retreat, *Geophys. Res. Lett.*, *35*(17),
 448 L17501, doi:10.1029/2008gl034457.
- 449 Hoppmann, M., et al. (2017), Ice platelets below Weddell Sea landfast sea ice, *Ann. Glaciol.*,
 450 *56*(69), 175-190, doi:10.3189/2015AoG69A678.
- 451 Hoppmann, M., M. E. Richter, I. J. Smith, S. Jendersie, P. J. Langhorne, N. D. Thomas, and G.
 452 S. Dieckmann (2020), Platelet ice, the Southern Ocean's hidden ice: a review, *Ann. Glaciol.*
- 453 Hunkeler, P. A., M. Hoppmann, S. Hendricks, T. Kalscheuer, and R. Gerdes (2016), A glimpse
 454 beneath Antarctic sea ice: Platelet layer volume from multifrequency electromagnetic induction
 455 sounding, *Geophys. Res. Lett.*, *43*(1), 222-231, doi:10.1002/2015gl065074.
- 456 Jeffries, M. O., K. Schwartz, K. Morris, A. D. Veazey, H. R. Krouse, and S. Gushing (1995),
 457 Evidence for platelet ice accretion in Arctic sea ice development, *Journal of Geophysical*
 458 *Research: Oceans*, *100*(C6), 10905-10914, doi:10.1029/95jc00804.
- 459 Katlein, C., P. Anhaus, I. Matero, and M. Nicolaus (2020a), Pressure, temperature, conductivity
 460 and dissolved oxygen raw data during ROV dives from POLARSTERN cruise PS122/2, links to
 461 files, edited, PANGAEA.
- 462 Katlein, C., P. M. Anhaus, Ilkka, and M. Nicolaus (2020b), Sea ice draft and acoustic backscatter
 463 (240kHz) raw data derived from multibeam sonar during the ROV BEAST dive PS122/2_18-19,
 464 edited, PANGAEA, doi:10.1594/PANGAEA.917498.
- 465 Katlein, C., P. Itkin, and D. V. Divine (2020c), Salinity measured on sea ice core PS122/2_24-
 466 114 during MOSAiC Leg 2, edited, PANGAEA, doi:10.1594/PANGAEA.919474.

- 467 Katlein, C., D. Krampe, and M. Nicolaus (2020d), Extracted frames from main ROV camera
468 videos during MOSAiC Leg 2, edited, PANGAEA, doi:10.1594/PANGAEA.919398.
- 469 Katlein, C., M. Schiller, H. J. Belter, V. Coppolaro, D. Wenslandt, and M. Nicolaus (2017), A
470 New Remotely Operated Sensor Platform for Interdisciplinary Observations under Sea Ice,
471 *Frontiers in Marine Science*, 4(281), doi:10.3389/fmars.2017.00281.
- 472 Kirillov, S., I. Dmitrenko, S. Rysgaard, D. Babb, J. Ehn, J. Bendtsen, W. Boone, D. Barber, and
473 N. Geilfus (2018), The Inferred Formation of a Subice Platelet Layer Below the Multiyear
474 Landfast Sea Ice in the Wandel Sea (NE Greenland) Induced by Meltwater Drainage, *Journal of*
475 *Geophysical Research: Oceans*, 123(5), 3489-3506, doi:10.1029/2017jc013672.
- 476 Knust, R. (2017), Polar Research and Supply Vessel POLARSTERN operated by the Alfred-
477 Wegener-Institute, *Journal of large-scale research facilities JLSRF*, 3, doi:10.17815/jlsrf-3-163.
- 478 Krumpen, T., et al. (2020), The MOSAiC ice floe: sediment-laden survivor from the Siberian
479 shelf, *The Cryosphere Discuss.*, 2020, 1-20, doi:10.5194/tc-2020-64.
- 480 Kwok, R., and D. A. Rothrock (2009), Decline in Arctic sea ice thickness from submarine and
481 ICESat records: 1958-2008, *Geophys. Res. Lett.*, 36, doi:10.1029/2009gl039035.
- 482 Kwok, R., G. Spreen, and S. Pang (2013), Arctic sea ice circulation and drift speed: Decadal
483 trends and ocean currents, *Journal of Geophysical Research: Oceans*, 118(5), 2408-2425,
484 doi:10.1002/jgrc.20191.
- 485 Langhorne, P. J., et al. (2015), Observed platelet ice distributions in Antarctic sea ice: An index
486 for ocean-ice shelf heat flux, *Geophys. Res. Lett.*, 42(13), 5442-5451,
487 doi:10.1002/2015gl064508.
- 488 Leonard, G. H., C. R. Purdie, P. J. Langhorne, T. G. Haskell, M. J. M. Williams, and R. D. Frew
489 (2006), Observations of platelet ice growth and oceanographic conditions during the winter of
490 2003 in McMurdo Sound, Antarctica, *Journal of Geophysical Research: Oceans*, 111(C4),
491 doi:10.1029/2005jc002952.
- 492 Lewis, E. L., and R. A. Lake (1971), Sea ice and supercooled water, *Journal of Geophysical*
493 *Research (1896-1977)*, 76(24), 5836-5841, doi:10.1029/JC076i024p05836.
- 494 Lewis, E. L., and A. R. Milne (1977), Underwater sea ice formation in "Polar Oceans," paper
495 presented at Proc. SCOR/SCAR Polar Oceans Conference, Arctic Institute North America.
- 496 Lewis, E. L., and R. G. Perkin (1983), Supercooling and energy exchange near the Arctic Ocean
497 surface, *Journal of Geophysical Research: Oceans*, 88(C12), 7681-7685,
498 doi:10.1029/JC088iC12p07681.
- 499 Lewis, E. L., and R. G. Perkin (1986), Ice pumps and their rates, *Journal of Geophysical*
500 *Research: Oceans*, 91(C10), 11756-11762, doi:10.1029/JC091iC10p11756.

- 501 Lofgren, G., and W. F. Weeks (2017), Effect of Growth Parameters on Substructure Spacing in
502 NaCl Ice Crystals, *J. Glaciol.*, 8(52), 153-164, doi:10.3189/S0022143000020827.
- 503 Mahoney, A. R., A. J. Gough, P. J. Langhorne, N. J. Robinson, C. L. Stevens, M. M. J. Williams,
504 and T. G. Haskell (2011), The seasonal appearance of ice shelf water in coastal Antarctica and its
505 effect on sea ice growth, *Journal of Geophysical Research: Oceans*, 116(C11),
506 doi:10.1029/2011jc007060.
- 507 Martin, S., and P. Kauffman (2006), The evolution of under-ice melt ponds, or double diffusion
508 at the freezing point, *Journal of Fluid Mechanics*, 64(3), 507-528,
509 doi:10.1017/S0022112074002527.
- 510 Notz, D., M. G. McPhee, M. G. Worster, G. A. Maykut, K. H. Schlünzen, and H. Eicken (2003),
511 Impact of underwater-ice evolution on Arctic summer sea ice, *Journal of Geophysical Research:*
512 *Oceans*, 108(C7), doi:10.1029/2001jc001173.
- 513 Pfirman, S., W. Haxby, H. Eicken, M. Jeffries, and D. Bauch (2004), Drifting Arctic sea ice
514 archives changes in ocean surface conditions, *Geophys. Res. Lett.*, 31(19), n/a-n/a,
515 doi:10.1029/2004GL020666.
- 516 Ragobert, T., et al. (2008), Tara : journey to the heart of the climate machine, edited.
- 517 Robinson, N. J., B. S. Grant, C. L. Stevens, C. L. Stewart, and M. J. M. Williams (2020),
518 Oceanographic observations in supercooled water: Protocols for mitigation of measurement
519 errors in profiling and moored sampling, *Cold Reg. Sci. Tech.*, 170, 102954,
520 doi:<https://doi.org/10.1016/j.coldregions.2019.102954>.
- 521 Rutter, J. W., and B. Chalmers (1953), A PRISMATIC SUBSTRUCTURE FORMED DURING
522 SOLIDIFICATION OF METALS, *Canadian Journal of Physics*, 31(1), 15-39, doi:10.1139/p53-
523 003.
- 524 Shokr, M., and N. Sinha (2015), *Sea Ice: Physics and Remote Sensing*, 1-579 pp.,
525 doi:10.1002/9781119028000.
- 526 Skogseth, R., F. Nilsen, and L. H. Smedsrud (2017), Supercooled water in an Arctic polynya:
527 observations and modeling, *J. Glaciol.*, 55(189), 43-52, doi:10.3189/002214309788608840.
- 528 Smith, I., P. Langhorne, T. Haskell, H. Trodahl, R. Frew, and R. Vennell (2001), Platelet ice and
529 the land-fast sea ice of McMurdo Sound, Antarctica, *Ann. Glaciol.*, 33, 21-27,
530 doi:10.3189/172756401781818365.
- 531 Thomas, D. N., and G. S. Dieckmann (2002), Biogeochemistry of Antarctic sea ice,
532 *Oceanography and marine biology*, 40, 143-170.
- 533 Tucker, W. B., A. J. Gow, D. A. Meese, H. W. Bosworth, and E. Reimnitz (1999), Physical
534 characteristics of summer sea ice across the Arctic Ocean, *Journal of Geophysical Research:*
535 *Oceans*, 104(C1), 1489-1504, doi:10.1029/98jc02607.

- 536 Vacchi, M., A. L. DeVries, C. W. Evans, M. Bottaro, L. Ghigliotti, L. Cutroneo, and E. Pisano
537 (2012), A nursery area for the Antarctic silverfish *Pleuragramma antarcticum* at Terra Nova Bay
538 (Ross Sea): first estimate of distribution and abundance of eggs and larvae under the seasonal
539 sea-ice, *Polar Biol.*, 35(10), 1573-1585, doi:10.1007/s00300-012-1199-y.
- 540 Weeks, W. F., and S. F. Ackley (1986), The Growth, Structure, and Properties of Sea Ice, in *The*
541 *Geophysics of Sea Ice*, edited by N. Untersteiner, pp. 9-164, Springer US, Boston, MA,
542 doi:10.1007/978-1-4899-5352-0_2.
- 543 WMO (2014), *JCOMM Expert Team on Sea Ice: Sea-Ice Nomenclature: snapshot of the WMO*
544 *Sea Ice Nomenclature WMO No. 259, volume I – Terminology and Codes; Volume II –*
545 *Illustrated Glossary and III – International System of Sea-Ice Symbols*, WMO-JCOMM, Geneva,
546 Switzerland, doi:<http://hdl.handle.net/11329/328>.
- 547 Wollenburg, J. E., M. Iversen, C. Katlein, T. Krumpfen, M. Nicolaus, G. Castellani, I. Peeken,
548 and H. Flores (2020), New observations of the distribution, morphology and dissolution
549 dynamics of cryogenic gypsum in the Arctic Ocean, *The Cryosphere*, 14(6), 1795-1808,
550 doi:10.5194/tc-14-1795-2020.
- 551 Zubov, N. N. (1963), Arctic ice.
552